

# Syntheses and X-ray Crystal Structures of the Tricobalt Mono(ethylidyne) Clusters $\text{Cp}^*_3\text{Co}_3(\mu_3\text{-CCH}_3)(\mu_3\text{-CO})(\mu_2\text{-H})$ , $\text{Cp}^*_3\text{Co}_3(\mu_3\text{-CCH}_3)(\mu_3\text{-CNCMe}_3)(\mu_2\text{-H})$ , and $\text{Cp}^*_3\text{Co}_3(\mu_3\text{-CCH}_3)(\mu_3\text{-NO})$

Charles P. Casey,\* Ross A. Widenhoefer, Susan L. Hallenbeck, and Randy K. Hayashi

Department of Chemistry, University of Wisconsin, Madison, Wisconsin 53706

Received December 28, 1993\*

$\text{Cp}^*_3\text{Co}_3(\mu_3\text{-CCH}_3)(\mu_3\text{-H})$  (**3**) reacted with CO to form the 1:1 carbonyl ethylidyne adduct  $\text{Cp}^*_3\text{Co}_3(\mu_3\text{-CCH}_3)(\mu_3\text{-CO})(\mu_2\text{-H})$  (**5**) in 82% yield. Similarly, *tert*-butyl isocyanide reacted with **3** to form the 1:1 isocyanide ethylidyne adduct  $\text{Cp}^*_3\text{Co}_3(\mu_3\text{-CCH}_3)(\mu_3\text{-CNCMe}_3)(\mu_2\text{-H})$  (**6**) in 87% yield. The reaction of **3** with NO formed the nitrosyl ethylidyne cluster  $\text{Cp}^*_3\text{Co}_3(\mu_3\text{-CCH}_3)(\mu_3\text{-NO})$  (**7**) in 84% yield. The structures of clusters **5**–**7** were determined by X-ray crystallography. Each cluster consists of an equilateral triangle of cobalt atoms symmetrically capped on one face by a  $\mu_3\text{-CCH}_3$  ligand and capped on the opposite face by a  $\mu_3\text{-CO}$  (**5**),  $\mu_3\text{-CNCMe}_3$  (**6**), or  $\mu_3\text{-NO}$  (**7**) ligand. Line shape analysis of the Cp\* peaks in the variable-temperature  $^1\text{H}$  NMR spectra of **5** and **6** allowed measurement of the barrier for migration of the hydride ligand between adjacent pairs of cobalt atoms in **5** [ $\Delta G^\ddagger = 10.3(1)$  kcal mol $^{-1}$ ] and **6** [ $\Delta G^\ddagger = 12.2(2)$  kcal mol $^{-1}$ ].

## Introduction

In collaboration with Theopold and co-workers, we recently reported the synthesis of the unusual tricobalt tetrahydride cluster  $\text{Cp}^*_3\text{Co}_3(\mu_2\text{-H})_3(\mu_3\text{-H})$  (**1**) and the dicobalt trihydride complex  $\text{Cp}^*_2\text{Co}_2(\mu\text{-H})_3$  from the reaction of  $[\text{Cp}^*\text{CoCl}]_2$  with  $\text{LiAlH}_4$  (Scheme 1).<sup>1</sup> Complex **1** is a reactive cluster due to its paramagnetic, 46-electron configuration and lack of bridging ligands other than hydrogen. For example, **1** reacted rapidly with CO at room temperature to form the dicarbonyl dihydride cluster  $\text{Cp}^*_3\text{Co}_3(\mu_3\text{-CO})(\mu_2\text{-CO})(\mu\text{-H})_2$ .<sup>2</sup> Reaction of **1** with NO occurred instantly to produce the trinuclear cluster  $\text{Cp}^*_3\text{Co}_3(\mu_3\text{-NO})_2$ .<sup>3</sup> The rapid insertion of *tert*-butyl isocyanide into a Co–H bond of **1** produced the formimidoyl cluster  $\text{Cp}^*_3\text{Co}_3(\mu\text{-H})(\mu_3\text{-}\eta^2\text{-HC=NCMe}_3)$ .<sup>2</sup>

We have also shown that **1** reacts with acetylene to form the mono(ethylidyne) clusters  $\text{Cp}^*_3\text{Co}_3(\mu_3\text{-CCH}_3)(\mu_2\text{-H})_3$  (**2**) and  $\text{Cp}^*_3\text{Co}_3(\mu_3\text{-CCH}_3)(\mu_3\text{-H})$  (**3**), which react further with acetylene to ultimately yield the bis(ethylidyne) cluster  $\text{Cp}^*_3\text{Co}_3(\mu_3\text{-CCH}_3)_2$  (**4**) (Scheme 2).<sup>4</sup> Clusters **2** and **3** interconvert cleanly via elimination or addition of  $\text{H}_2$ . Their rate of interconversion is much slower than their rate of formation from reaction of **1** with acetylene. Pardy and co-workers had previously reported the isolation of a tricobalt cluster from the thermolysis of  $\text{Cp}^*\text{Co}(\text{H}_2\text{C=CH}_2)_2$  which they formulated as  $\text{Cp}^*_3\text{Co}_3(\mu_3\text{-CCH}_3)_2$  on the basis of an X-ray crystal structure.<sup>5</sup> However, our X-ray crystallographic analysis of clusters **3** and **4** revealed that Pardy's cluster was actually the mirror-disordered mono(ethylidyne) cluster **3**, not the bis(ethylidyne) cluster **4**.<sup>6</sup>

The mono(ethylidyne) monohydride cluster **3** is analogous to the tetrahydride cluster **1** in that both clusters possess an open-shell, 46-electron configuration and at least one reactive hydride

ligand. Because cluster **1** was reactive toward CO,<sup>2</sup> *tert*-butyl isocyanide,<sup>2</sup> and NO,<sup>3</sup> we anticipated that cluster **3** might also react with these molecules to form new mono(ethylidyne) tricobalt derivatives. Here we report that **3** reacts rapidly with CO and with *tert*-butyl isocyanide to form the 1:1 adducts  $\text{Cp}^*_3\text{Co}_3(\mu_3\text{-CCH}_3)(\mu_3\text{-CO})(\mu_2\text{-H})$  (**5**) and  $\text{Cp}^*_3\text{Co}_3(\mu_3\text{-CCH}_3)(\mu_3\text{-CNCMe}_3)(\mu_2\text{-H})$  (**6**). The reaction of **3** with NO produced the nitrosyl ethylidyne cluster  $\text{Cp}^*_3\text{Co}_3(\mu_3\text{-CCH}_3)(\mu_3\text{-NO})$  (**7**) with loss of a hydride ligand.

## Results and Discussion

**Synthesis of Tricobalt Mono(ethylidyne) Derivatives.** When a benzene solution of **3** was stirred under 1 atm of CO, the color immediately changed from brown to red. Evaporation of solvent and crystallization from toluene gave the 1:1 carbonyl adduct  $\text{Cp}^*_3\text{Co}_3(\mu_3\text{-CCH}_3)(\mu_3\text{-CO})(\mu_2\text{-H})$  (**5**) in 82% yield (Scheme 3). Cluster **5** was characterized by spectroscopy and by single-crystal X-ray diffraction. In the  $^1\text{H}$  NMR spectrum, resonances at  $\delta$  3.73 and  $-\text{27.8}$  established a 1:1 ratio of ethylidyne to hydride ligands. At room temperature, a single sharp resonance for the Cp\* ligands was observed at  $\delta$  1.63; when the sample was cooled to  $-75$  °C, a 1:2 ratio of Cp\* resonances was seen at  $\delta$  1.80 and 1.62. In the IR spectrum (KBr), a strong absorbance at 1684  $\text{cm}^{-1}$  indicated that the CO ligand was triply bridged. The IR spectrum of **5** also displayed a very weak band at 1520  $\text{cm}^{-1}$  which was replaced by a broad shoulder at  $\sim 1080$   $\text{cm}^{-1}$  in the spectrum of the deuterated isotopomer  $\text{Cp}^*_3\text{Co}_3(\mu_3\text{-CCH}_3)(\mu_3\text{-CO})(\mu_2\text{-D})$ ;<sup>7</sup> this band provides evidence for a doubly bridged hydride ligand. The low-frequency chemical shift of the hydride ligand in the  $^1\text{H}$  NMR spectrum<sup>8</sup> is also consistent with a hydride ligand that is doubly bridged rather than terminally bound. The

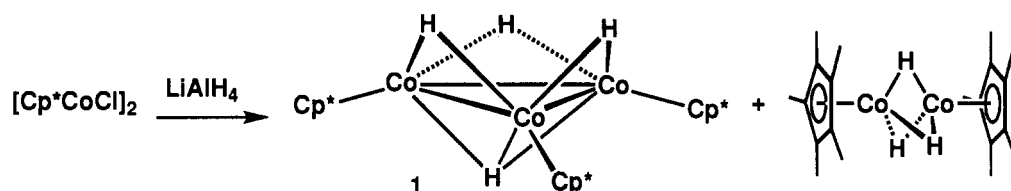
\* Abstract published in *Advance ACS Abstracts*, May 1, 1994.

- (1) Kersten, J. L.; Rheingold, A. L.; Theopold, K. H.; Casey, C. P.; Widenhoefer, R. A.; Hop, C. E. *Angew. Chem.* **1992**, *104*, 1364; *Angew. Chem., Int. Ed. Engl.* **1992**, *32*, 1341.
- (2) Casey, C. P.; Widenhoefer, R. A.; Hallenbeck, S. L.; Gavney, J. A., Jr. *J. Chem. Soc., Chem. Commun.* **1993**, 1692.
- (3) Casey, C. P.; Widenhoefer, R. A.; Hayashi, R. K. *Inorg. Chim. Acta* **1993**, *212*, 81.
- (4) Casey, C. P.; Widenhoefer, R. A.; Hallenbeck, S. L. *Organometallics* **1993**, *12*, 3788.
- (5) Pardy, R. B. A.; Smith, G. W.; Vickers, M. E. *J. Organomet. Chem.* **1983**, *252*, 341.
- (6) Casey, C. P.; Widenhoefer, R. A.; Hallenbeck, S. L.; Hayashi, R. K.; Powell, D. R.; Smith, G. W. *Organometallics* **1994**, *13*, 1521.

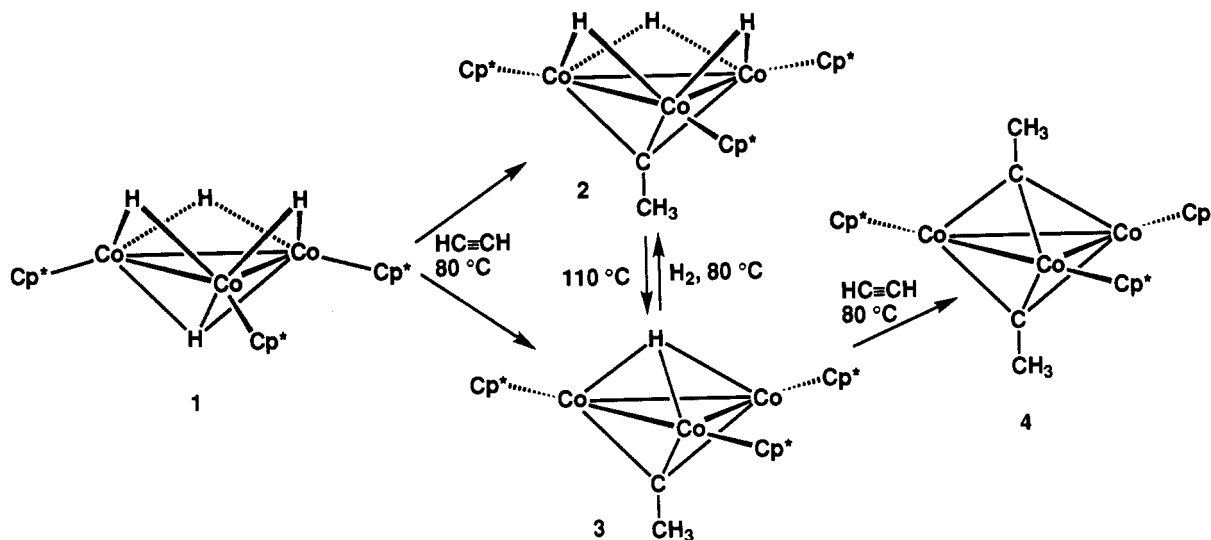
(7) Casey, C. P.; Widenhoefer, R. A.; Hallenbeck, S. L. Unpublished results.

(8) The chemical shifts of terminal cobalt hydrides are normally between  $\delta$   $-10$  and  $\delta$   $-20$ : (a) Pères, Y.; Dartiguenave, M.; Dartiguenave, Y.; Britten, J. F.; Beauchamp, A. L. *Organometallics* **1990**, *9*, 1041. (b) Werner, H.; Hofmann, W. *Angew. Chem., Int. Ed. Engl.* **1977**, *16*, 794. (c) Werner, H.; Buchner, W.; Hofmann, W. *Angew. Chem., Int. Ed. Engl.* **1977**, *16*, 796. (d) Werner, H.; Hofmann, W. *Chem. Ber.* **1977**, *110*, 3481. (e) Werner, H.; Hofmann, W. *Angew. Chem., Int. Ed. Engl.* **1979**, *18*, 158. (f) Werner, H.; Hofmann, W. *Chem. Ber.* **1981**, *114*, 2681. (g) Werner, H.; Heiser, B.; Klingert, B.; Dörfel, R. *J. Organomet. Chem.* **1982**, *240*, 179. (h) Kesz, H. D.; Saillant, R. B. *Chem. Rev.* **1972**, *72*, 231 and references therein.

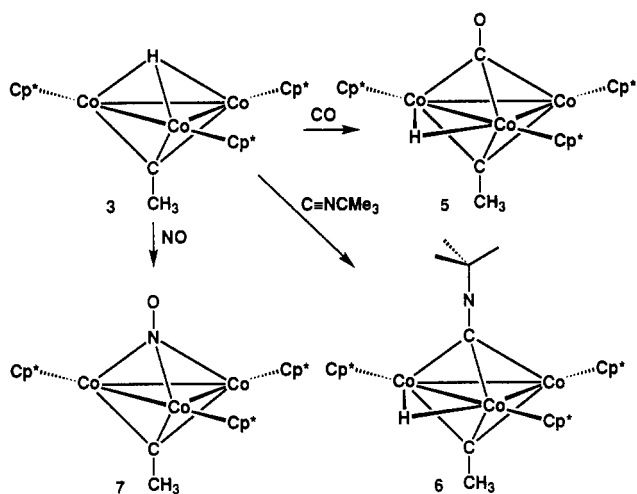
Scheme 1



Scheme 2



Scheme 3



strong tendency of hydride ligands to adopt bridging positions in metal clusters has been previously observed.<sup>9</sup>

**3** reacted rapidly with excess *tert*-butyl isocyanide in benzene at room temperature to form the 1:1 isocyanide adduct  $\text{Cp}^*_3\text{-Co}_3(\mu_3\text{-CCH}_3)(\mu_3\text{-CNCMe}_3)(\mu_2\text{-H})$  (**6**) in 87% yield as a black powder (Scheme 3). Cluster **6** was characterized by spectroscopy and by X-ray crystallography. The  $^1\text{H}$  NMR spectrum of **6** displayed resonances at  $\delta$  4.81 and  $-27.6$  which established a 1:1 ratio of ethylidyne to hydride ligands. The very low frequency of the hydride resonance of **6** is consistent with a doubly bridged hydride. At room temperature, a single resonance for the Cp\* ligands was observed at  $\delta$  1.64; when the sample was cooled to  $-50^\circ\text{C}$ , a 1:2 ratio of Cp\* resonances was seen at  $\delta$  1.74 and 1.64.

Exposure of a benzene- $d_6$  solution of **3** to excess NO (1 atm) at room temperature led to destruction of the cluster and formation of a black precipitate and a yellow solution which displayed no

Cp\* resonances in the  $^1\text{H}$  NMR spectrum. However, reaction of **3** with 1 equiv of NO in benzene at room temperature led to the isolation of the nitrosyl ethylidyne cluster  $\text{Cp}^*_3\text{Co}_3(\mu_3\text{-CCH}_3)(\mu_3\text{-NO})$  (**7**) in an 84% yield as a red powder (Scheme 3). Cluster **7** was characterized by spectroscopy and by X-ray crystallography. In the IR spectrum, a single  $\mu_3\text{-NO}$  absorbance was observed at  $1374\text{ cm}^{-1}$ , in the normal range for  $\mu_3\text{-NO}$  clusters.<sup>10,11</sup>

The conversions of **3** to clusters **5**–**7** were all rapid and clean. The reactions of **3** with CO, CNCMe<sub>3</sub>, and NO were all complete within 1 min at room temperature. No other products were observable by  $^1\text{H}$  NMR spectroscopy. Attempts to determine yields by NMR using an internal standard were complicated by the unreliable integration of the paramagnetic resonance of **3**;<sup>12</sup> apparent NMR yields ranged from 125 to 140%.

Clusters **5**–**7** possess a high degree of thermal stability. For example,  $^1\text{H}$  NMR analysis ( $\text{C}_6\text{Me}_6$  internal standard) showed <20% decomposition of **5** after 5 days at  $120^\circ\text{C}$  in benzene- $d_6$ . Similarly, clusters **6** and **7** exhibited no detectable decomposition (<5%) over 5 days at  $110^\circ\text{C}$  in benzene- $d_6$ .

**X-ray Crystallography of Mono(ethylidyne) Clusters.** The structures of clusters **5** (Figure 1, Tables 1 and 2), **6** (Figure 2, Tables 1 and 3), and **7** (Figure 3, Tables 1 and 4) were determined by X-ray crystallography. Preliminary analysis of **5** and **7** revealed that the  $\mu_3$  ligands of these clusters were necessarily disordered under the crystallographic site symmetry ( $3/m$ ). As a result,

(9) Muetterties, E. L.; Rhodin, T. N.; Band, E.; Brucker, C. F.; Pretzer, W. *R. Chem. Rev.* **1979**, *79*, 91.

- (10) (a) King, R. B.; Bisnette, M. B. *Inorg. Chem.* **1964**, *3*, 791. (b) Elder, R. C.; Cotton, F. A.; Schunn, R. A. *J. Am. Chem. Soc.* **1967**, *89*, 3645. (c) Elder, R. C. *Inorg. Chem.* **1974**, *13*, 1037. (d) Kolthammer, B. W. S.; Legzdins, P. *J. Chem. Soc., Dalton Trans.* **1978**, 31. (e) Müller, J.; Sonn, I.; Akhnouk, T. *J. Organomet. Chem.* **1989**, *367*, 133. (f) Dimas, P. A.; Lawson, R. J.; Shapley, J. R. *Inorg. Chem.* **1981**, *20*, 281. (g) Müller, J.; Manzoni, G.; Sonn, I. *J. Organomet. Chem.* **1988**, *340*, C15. (h) Müller, J.; Sonn, I.; Akhnouk, T. *J. Organomet. Chem.* **1991**, *414*, 381.
- (11) (a) Müller, J.; Schmitt, S. *J. Organomet. Chem.* **1975**, *97*, C54. (b) Kubat-Martin, K. A.; Spencer, B.; Dahl, L. F. *Organometallics* **1987**, *6*, 2580. (c) Kubat-Martin, K. A.; Rae, A. D.; Dahl, L. F. *Organometallics* **1985**, *4*, 2221. (d) Bedard, R. L.; Rae, A. D.; Dahl, L. F. *J. Am. Chem. Soc.* **1986**, *108*, 5924. (e) Bedard, R. L.; Dahl, L. F. *J. Am. Chem. Soc.* **1986**, *108*, 5942.
- (12) Theopold, K. H. *Acc. Chem. Res.* **1990**, *23*, 263.

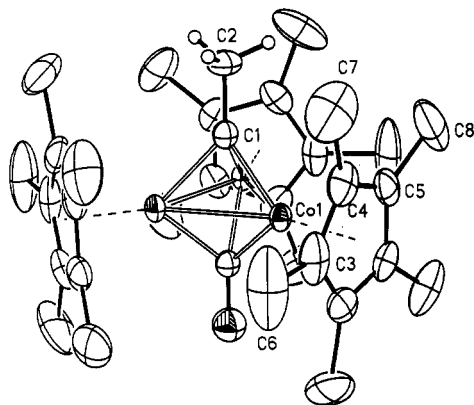


Figure 1. X-ray crystal structure for  $\text{Cp}^*_3\text{Co}_3(\mu_3\text{-CCH}_3)(\mu_3\text{-CO})(\mu_2\text{-H})$  (5).

Table 1. Crystal Structure Data for  $\text{Cp}^*_3\text{Co}_3(\mu_3\text{-CCH}_3)(\mu_3\text{-CO})(\mu_2\text{-H})$  (5),  $\text{Cp}^*_3\text{Co}_3(\mu_3\text{-CCH}_3)(\mu_3\text{-CNCMe}_3)(\mu_2\text{-H}) \cdot 1/2\text{C}_5\text{H}_{12}$  (6), and  $\text{Cp}^*_3\text{Co}_3(\mu_3\text{-CCH}_3)(\mu_3\text{-NO})$  (7)

	5	6	7
empirical formula	$\text{C}_{33}\text{H}_{49}\text{OC}_3$	$\text{C}_{37}\text{H}_{58}\text{NOC}_3$	$\text{C}_{32}\text{H}_{57}\text{NOC}_3$
color; habit	black block	black plate	black plate
crystal size (mm)	$0.5 \times 0.3 \times 0.3$	$0.5 \times 0.3 \times 0.1$	$0.6 \times 0.5 \times 0.05$
crystal system	hexagonal	triclinic	hexagonal
space group	$P6_3/m$	$P\bar{1}$	$P6_3/m$
unit cell dimens			
$a$ (Å)	10.6943(6)	10.797(1)	10.6760(4)
$b$ (Å)		10.8581(9)	
$c$ (Å)	15.431(4)	19.221(1)	15.457(4)
$\alpha$ (deg)		76.597(7)	
$\beta$ (deg)		89.619(7)	
$\gamma$ (deg)		60.429(7)	
$V$ (Å <sup>3</sup> )	1528.4(4)	1891.0(3)	1525.7(4)
no. of peaks to determine cell	52	38	45
$2\theta$ range of cell peaks (deg)	9.0–25.0	10.0–25.0	10.0–25.0
$Z$	2	2	2
fw	638.5	729.7	639.5
density (calc) (g cm <sup>-3</sup> )	1.387	1.282	1.392
abs coeff (mm <sup>-1</sup> )	1.630	1.324	1.634
$F(000)$	672	778	672
$R(F)$ (%)	3.22	4.63	5.30
$R_w(F)$ (%)	4.64	6.09	6.61

Table 2. Selected Bond Lengths (Å) and Angles (deg) for  $\text{Cp}^*_3\text{Co}_3(\mu_3\text{-CCH}_3)(\mu_3\text{-CO})(\mu_2\text{-H})$  (5)

Co(1)–Co(1a)	2.425(1)	Co(1)–C(5)	2.097(4)
Co(1)–C(1)	1.914(3)	Co(1)–Co(1a)–Co(1b)	60.0(1)
Co(1)–C(1a)	1.914(3)	Co(1)–C(1)–C(2)	133.0(1)
C(1)–C(2)	1.38(6)	Co(1)–C(1)–O(1)	133.0(1)
C(1a)–O(1)	1.29(4)	C(1)–Co(1)–C(1a)	86.0(2)
Co(1)–C(3)	2.121(4)	Co(1)–C(1)–Co(1a)	78.6(2)
Co(1)–C(4)	2.118(3)		

each cluster was refined according to a mirror-disordered model which assigned full-weight to a common apical atom and half-weight to the ethylidyne methyl group and the oxygen atom (see Experimental Section). The mirror disorder of the  $\mu_3$  ligands in clusters 5 and 7 is similar to disorder of the  $\mu_3\text{-H}$  and the  $\mu_3\text{-CCH}_3$  ligands observed in cluster 3.<sup>6</sup>

The structures of CO derivative 5 and NO derivative 7 are nearly identical. Each cluster consists of an equilateral triangle of three cobalt atoms symmetrically capped on one face by a  $\mu_3\text{-CCH}_3$  ligand and symmetrically capped on the opposite face by either a  $\mu_3\text{-CO}$  (5) or a  $\mu_3\text{-NO}$  (7) ligand; the hydride ligand in 5 was not observed crystallographically. The six symmetry-equivalent Co– $\mu_3\text{-C}$  distances [1.914(3) Å] in 5 and the six equivalent Co– $\mu_3\text{-X}$  (X = C, N) distances [1.856(4) Å] in 7 are within the range observed for other tricobalt clusters possessing

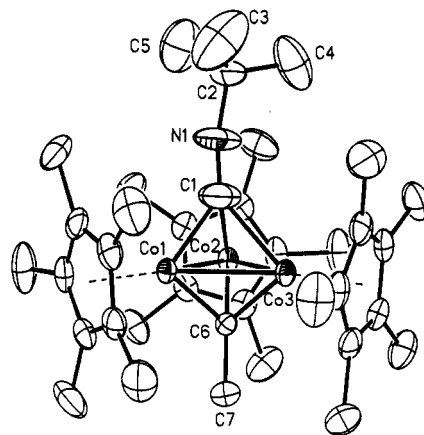


Figure 2. X-ray crystal structure for  $\text{Cp}^*_3\text{Co}_3(\mu_3\text{-CCH}_3)(\mu_3\text{-CNCMe}_3)(\mu_2\text{-H})$  (6).

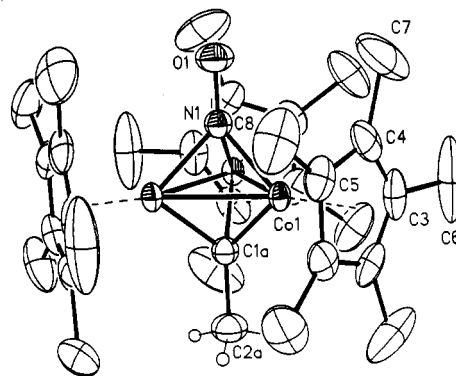


Figure 3. X-ray crystal structure for  $\text{Cp}^*_3\text{Co}_3(\mu_3\text{-CCH}_3)(\mu_3\text{-NO})$  (7).

Table 3. Selected Bond Lengths (Å) and Angles (deg) for  $\text{Cp}^*_3\text{Co}_3(\mu_3\text{-CCH}_3)(\mu_3\text{-CNCMe}_3)(\mu_2\text{-H})$  (6)

Co(1)–Co(2)	2.476(1)	Co(1)–C(1)–N(1)	136(1)
Co(1)–Co(3)	2.478(1)	Co(2)–C(1)–N(1)	137.1(7)
Co(2)–Co(3)	2.479(1)	Co(3)–C(1)–N(1)	136.8(9)
Co(1)–C(1)	1.960(9)	Co(1)–C(6)–C(7)	130.1(4)
Co(2)–C(1)	2.139(6)	Co(2)–C(6)–C(7)	129.8(2)
Co(3)–C(1)	2.159(9)	Co(3)–C(6)–C(7)	130.3(4)
Co(1)–C(6)	1.867(5)	C(1)–Co(1)–C(6)	90.5(3)
Co(2)–C(6)	1.871(4)	C(1)–Co(2)–C(6)	85.1(2)
Co(3)–C(6)	1.867(4)	C(1)–Co(3)–C(6)	84.6(3)
C(1)–N(1)	1.196(8)	C(1)–N(1)–C(2)	165(1)
N(1)–C(2)	1.374(8)		

Table 4. Selected Bond Lengths (Å) and Angles (deg) for  $\text{Cp}^*_3\text{Co}_3(\mu_3\text{-CCH}_3)(\mu_3\text{-NO})$  (7)

Co(1)–Co(1a)	2.408(1)	Co(1)–C(4)	2.105(5)
Co(1)–C(1)	1.856(4)	Co(1)–C(5)	2.089(6)
Co(1)–N(1)	1.856(4)	Co(1)–C(1)–C(2)	131.5(1)
C(1)–C(2)	1.5(1)	Co(1)–N(1)–O(1)	131.5(1)
N(1)–O(1)	1.25(6)	C(1)–Co(1)–N(1)	83.0(3)
Co(1)–C(3)	2.117(6)	Co(1)–C(1)–Co(1a)	80.9(2)

$\mu_3\text{-alkylidyne}$ ,<sup>13</sup>  $\mu_3\text{-CO}$ ,<sup>11d,e,14</sup> or  $\mu_3\text{-NO}$ <sup>11</sup> ligands. The Cp\* ligands in 5 and 7 are arranged head to tail about the cobalt triangle with one Cp\* methyl group [C(6)] in the Co<sub>3</sub> plane. The Co–Co

- (13) (a) Wadepohl, H.; Pritzkow, H. *Polyhedron* 1989, 8, 1939. (b) Fritch, J. R.; Vollhardt, K. P. C.; Thompson, M. R.; Day, V. W. *J. Am. Chem. Soc.* 1979, 101, 2768. (c) Yamazaki, H.; Wakatsuki, Y.; Aoki, K. *Chem. Lett.* 1979, 1041. (d) Stella, S.; Floriani, C.; Chiesi-Villa, A.; Guastini, C. *New J. Chem.* 1988, 12, 621. (e) Sappa, E.; Tiripicchio, A.; Braunstein, P. *Chem. Rev.* 1983, 83, 215.
- (14) (a) Uchtman, V. A.; Dahl, L. F. *J. Am. Chem. Soc.* 1969, 91, 3763. (b) Bailey, W. I.; Cotton, F. A.; Jamerson, J. D.; Kolthammer, B. W. *Inorg. Chem.* 1982, 21, 3131. (c) Olson, W. L.; Stacy, A. M.; Dahl, L. F. *J. Am. Chem. Soc.* 1986, 108, 7646. (d) Olson, W. L.; Dahl, L. F. *J. Am. Chem. Soc.* 1986, 108, 7657. (e) Ziebarth, M. S.; Dahl, L. F. *J. Am. Chem. Soc.* 1990, 112, 2411. (f) Barnes, C. E.; Orvis, J. A.; Staley, D. L.; Rheingold, A. L.; Johnson, D. C. *J. Am. Chem. Soc.* 1989, 111, 4992.

distance in **5** is very similar to the distances observed for the 48-electron bicapped  $\text{Cp}^*_3\text{Co}_3$  clusters  $\text{Cp}^*_3\text{Co}_3(\mu_3\text{-CO})(\mu_3\text{-NH})$  (2.428 Å),<sup>11d</sup>  $\text{Cp}^*_3\text{Co}_3(\mu_3\text{-NO})_2$  (2.423 Å),<sup>3</sup> and  $\text{Cp}^*_3\text{Co}_3(\mu_3\text{-CCH}_3)_2$  (2.437 Å).<sup>6</sup> The Co–Co distance for cluster **7** [2.408(1) Å] is 0.017 Å shorter than the distance observed in cluster **5** and is unusually short for a 48-electron  $\text{Cp}^*_3\text{Co}_3$  bicapped cluster.

Because of the very high  $3/m$  symmetry seen in the crystal structure of **5**, no direct information about the position of the  $\mu$ -hydride ligand or about the difference between the Co– $\mu$ -H–Co and Co–Co distances can be made. However, the  $\mu_2$ -hydride ligand is probably positioned very near the  $\text{Co}_3$  plane to minimize steric interaction with the apical carbon atoms; if it were not, one of the two  $\mu_3$ -ligands would have been displaced from the 3-fold axis and would have broken the crystal symmetry. Similarly, if the Co– $\mu$ -H–Co and Co–Co distances were not very similar, the crystal symmetry would also have been broken.

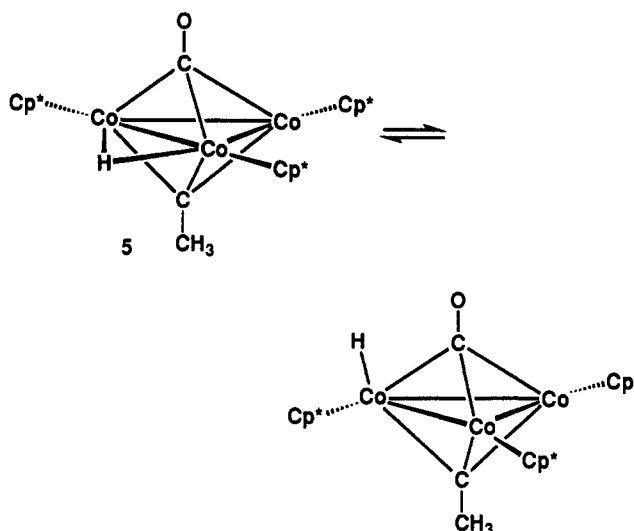
In contrast to clusters **5** and **7**, cluster **6** lacks both a crystallographic mirror plane and a 3-fold axis. Cluster **6** consists of a nearly equilateral triangular array of three cobalt atoms capped on one face by a  $\mu_3$ -CCH<sub>3</sub> ligand and capped on the opposite face by a  $\mu_3$ -CNCMe<sub>3</sub> ligand; the hydride ligand was not observed crystallographically. The Cp\* ligands are arranged head to tail about the  $\text{Co}_3$  triangle with the centroids of each Cp\* ligand displaced out of the  $\text{Co}_3$  plane away from the bulky *tert*-butyl group by an average of 0.12 Å. The three Co– $\mu_3$ -CCH<sub>3</sub> distances range from 1.867(5) to 1.871(4) Å and are similar to the values observed for clusters **5** and **7**.

The isocyanide ligand is distorted away from a symmetric triple-bridged arrangement with one short [Co(1)–C(1) = 1.960(9) Å] and two long Co– $\mu_3$ -CNCMe<sub>3</sub> distances [Co(2)–C(1) = 2.139(6) Å, Co(3)–C(1) = 2.159(9) Å]. The C(1)–N(1)–C(2) angle [165(1)°] is displaced slightly from linearity and bends away from Co(1). The slight bend in the C–N–C bond appears to compensate for the asymmetric  $\mu_3$ -bonding of the isocyanide ligand and approximately centers the C(2) carbon of the *tert*-butyl group over the  $\text{Co}_3$  triangle.

The slight distortion of the isocyanide ligand away from symmetric  $\mu_3$ -bonding suggests that the hydride ligand bridges the Co(2)–Co(3) bond. Normally, M– $\mu$ -H–M bonds are somewhat longer than M–M bonds.<sup>15</sup> However, the Co(2)–Co(3) distance [2.479(1) Å] is not significantly longer than either the Co(1)–Co(2) [2.476(1) Å] or Co(1)–Co(3) [2.478(1) Å] distance. The equivalence of the three Co–Co distances in cluster **6** may result from the resistance of the  $\mu_3$ -ethynylidene ligand to bond to the metals in an unsymmetric manner. The average Co–Co distance for **6** [2.477(1) Å] is somewhat longer than the Co–Co distances observed for **5** and **7** but is nearly identical to the Co–Co distance observed for the dicarbonyl dihydride cluster  $\text{Cp}^*_3\text{Co}_3(\mu_3\text{-CO})(\mu_2\text{-CO})(\mu\text{-H})_2$  [2.446(1) Å].<sup>16</sup>

Although there are numerous clusters possessing  $\mu_3$ -CO ligands, the only examples of clusters possessing triply bridged isocyanide ligands are  $\text{Ni}_4(\text{CNCMe}_3)_7$ ,<sup>17</sup>  $\text{Fe}_3(\text{CO})_9(\mu_3\text{-}\eta^2\text{-CNCMe}_3)$ ,<sup>18</sup> and  $\text{Fe}_3(\text{CO})_8(\mu_3\text{-}\eta^2\text{-CNCMe}_3)\text{L}$  [L = P(OMe)<sub>3</sub>, P(OEt)<sub>3</sub>, PMe<sub>3</sub>, PEt<sub>3</sub>],<sup>19</sup> and in each of these cases, the  $\mu_3$ -isocyanide is bonded to the metals through both the carbon and nitrogen atoms. Therefore, **6** is the first structurally characterized cluster containing a  $\mu_3$ -isocyanide ligand bonded through only the terminal carbon atom.

Scheme 4



**Variable-Temperature <sup>1</sup>H NMR Spectroscopy of **5** and **6**.** The presence of a symmetry-breaking  $\mu_2$ -H ligand in **5** was inferred from the observation of a 1:2 ratio of Cp\* resonances at  $\delta$  1.80 and 1.62 in the <sup>1</sup>H NMR spectrum of **5** in toluene-*d*<sub>8</sub> (500 MHz) at –75 °C. At room temperature, a single sharp resonance for the Cp\* ligands was observed at  $\delta$  1.63. As the temperature was lowered, the Cp\* resonance broadened and coalesced at –60 °C. The resonances for the hydride ligand ( $\delta$  –27.8) and the ethynylidene methyl group ( $\delta$  3.73) remained unchanged over this temperature range.

The variable-temperature <sup>1</sup>H NMR spectrum of cluster **5** is consistent with migration of the  $\mu$ -H ligand between adjacent pairs of cobalt atoms via a terminal hydride intermediate (Scheme 4). This process creates a time-averaged 3-fold symmetry axis perpendicular to the tricobalt plane. A barrier for migration of the hydride ligand between adjacent cluster edges of  $\Delta G^\ddagger = 10.3$ –(1) kcal mol<sup>–1</sup> at 213 K was calculated from a complete <sup>1</sup>H NMR line shape analysis of the Cp\* resonances of **5** over the temperature range from –80 to –50 °C (Figure 4). Similar bridging hydride to terminal hydride interconversions have been proposed to explain fluxional hydride behavior in Os<sub>3</sub>,<sup>20</sup> Ru<sub>3</sub>,<sup>21</sup> and Ru<sub>4</sub><sup>22</sup> clusters.

In the 500-MHz <sup>1</sup>H NMR spectrum of **6** at –50 °C, a 1:2 ratio of Cp\* resonances was observed at  $\delta$  1.74 and 1.64. This is consistent with the presence of a  $\mu_2$ -H ligand and with the low symmetry seen by X-ray crystallography. At room temperature, a single sharp resonance for the Cp\* ligands was observed at  $\delta$  1.64. As the temperature was lowered, the Cp\* resonances broadened and coalesced at –31 °C. The resonances for the cobalt hydride ( $\delta$  –27.2), the ethynylidene methyl group ( $\delta$  4.81), and the *tert*-butyl group ( $\delta$  1.82) remained unchanged over this temperature range.

The variable-temperature <sup>1</sup>H NMR spectrum of cluster **6** is consistent with migration of a  $\mu$ -H ligand between adjacent pairs of cobalt atoms via a terminal hydride intermediate. The barrier for migration of the hydride ligand between adjacent cluster edges of  $\Delta G^\ddagger = 12.2$ (2) kcal mol<sup>–1</sup> at 242 K was calculated from a complete <sup>1</sup>H NMR line shape analysis of the Cp\* resonances of **6** over the temperature range from –50 to –25 °C.

## Experimental Section

**General Methods.** All manipulations were performed under a nitrogen atmosphere in an inert-atmosphere glovebox or by standard high-vacuum

(15) Collman, J. P.; Hegedus, L. S.; Norton, J. R.; Finke, R. G. *Principles and Applications of Organotransition Metal Chemistry*, 2nd ed.; University Science Books: Mill Valley, CA, 1987; p 83.

(16) Casey, C. P.; Widenhoefer, R. A.; Hallenbeck, S. L.; Hayashi, R. K. Unpublished results.

(17) Day, V. W.; Day, R. O.; Kristoff, J. S.; Hirsekorn, F. J.; Muetterties, E. L. *J. Am. Chem. Soc.* **1975**, *97*, 2571.

(18) (a) Bruce, M. I.; Hambley, T. W.; Nicholens, B. K. *J. Chem. Soc., Chem. Commun.* **1982**, 353. (b) Bruce, M. I.; Hambley, T. W.; Nicholens, B. K.; *J. Chem. Soc., Dalton Trans.* **1983**, 2385.

(19) Lentz, D.; Marschall, R. *Chem. Ber.* **1990**, *124*, 497.

(20) Keister, J. B.; Shapley, J. R. *Inorg. Chem.* **1982**, *21*, 3304.

(21) (a) Churchill, M. R.; Janik, T. S.; Duggan, T. P.; Keister, J. B. *Organometallics* **1987**, *6*, 799. (b) Nevinger, L. R.; Keister, J. B. *Organometallics* **1990**, *9*, 2312.

(22) Shapley, J. R.; Richter, S. I.; Churchill, M. R.; Lashewycz, R. A. *J. Am. Chem. Soc.* **1977**, *99*, 7384.

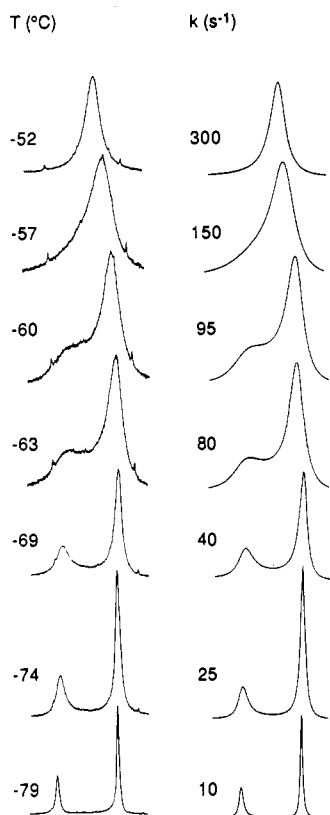


**Figure 4.** 500-MHz variable-temperature  $^1\text{H}$  NMR spectra of the  $\text{Cp}^*$  region of **5**. Observed spectra and temperature are on the left. Simulated spectra and rates are on the right.

techniques.  $^1\text{H}$  NMR spectra were obtained on a Bruker WP200 or AM500 spectrometer, and  $^{13}\text{C}$  NMR spectra were obtained on a Bruker AM500 (126 MHz) spectrometer. Probe temperatures were measured with a platinum resistance wire and are assumed to be accurate to  $\pm 1$   $^\circ\text{C}$ . Line shape analyses were performed employing the program DNMR5.<sup>23</sup> Infrared spectra were recorded on a Mattson Polaris FT-IR spectrometer. Mass spectra were determined on a Kratos MS-80 spectrometer. Elemental analyses were performed by Desert Analytics (Tucson, AZ). Diethyl ether, hexane, pentane, and benzene were distilled from sodium and benzophenone; toluene was distilled from sodium. Benzene- $d_6$  and toluene- $d_8$  were distilled from sodium and benzophenone or from sodium-potassium alloy. *tert*-Butyl isocyanide (Fluka), CO (Airco), and NO (Liquid Carbonics) were used as received.

**$\text{Cp}^*_3\text{Co}_3(\mu_3\text{-CCH}_3)(\mu_3\text{-CO})(\mu_2\text{-H})$  (**5**).** A brown solution of  $\text{Cp}^*_3\text{Co}_3(\mu_3\text{-CCH}_3)(\mu_3\text{-H})$  (**3**) (50 mg, 0.084 mmol) in benzene (10 mL) was stirred under CO (1 atm) for 30 min to form a red solution. Benzene and unreacted CO were evaporated under vacuum, and the residue was crystallized from toluene at  $-20$   $^\circ\text{C}$  to give **5** (43 mg, 82%) as red needles:  $^1\text{H}$  NMR ( $\text{C}_6\text{D}_6$ , 200 MHz)  $\delta$  3.73 ( $\mu_3\text{-CCH}_3$ ), 1.64 ( $\text{C}_5\text{Me}_5$ ),  $-26.78$  (Co- $\mu\text{-H}$ );  $^{13}\text{C}\{^1\text{H}\}$  NMR ( $\text{C}_6\text{D}_6$ , 126 MHz,  $^{13}\text{CO}$  isotopomer)  $\delta$  267.3 (CO), 94.3 ( $\text{C}_5\text{Me}_5$ ), 42.2 ( $\mu_3\text{-CCH}_3$ ), 10.5 ( $\text{C}_5\text{Me}_5$ ),  $\mu_3\text{-CCH}_3$  carbon not observed; IR (THF) 1671  $\text{cm}^{-1}$ ; IR (KBr) 1684 (vs,  $\nu(\text{CO})$ ), 1516 (vw,  $\nu(\text{Co-H})$ )  $\text{cm}^{-1}$ ; HRMS (EI) calcd (found) for  $\text{C}_{33}\text{H}_{49}\text{OC}_3$  638.1776 (638.1757). Anal. Calcd (found) for  $\text{C}_{33}\text{H}_{49}\text{OC}_3$ : C, 62.07 (62.14); H, 7.73 (7.76).

**$\text{Cp}^*_3\text{Co}_3(\mu_3\text{-CCH}_3)(\mu_3\text{-CNCMe}_3)(\mu_2\text{-H})$  (**6**).** *tert*-Butyl isocyanide (35 mg, 0.42 mmol) and **3** (25 mg, 0.04 mmol) in benzene (6 mL) were stirred for 1 h. Benzene and unreacted  $\text{CNCMe}_3$  were evaporated under vacuum, and the residue was extracted with pentane. The pentane extract was filtered through Celite, and the filtrate was evaporated under vacuum to give  $\text{Cp}^*_3\text{Co}_3(\mu_3\text{-CCH}_3)(\mu_3\text{-CNCMe}_3)(\mu_2\text{-H})$  (**6**) (26 mg, 86%) as a black powder which was  $>95\%$  pure by  $^1\text{H}$  NMR analysis. **6** was further purified by crystallization from pentane at  $-20$   $^\circ\text{C}$ :  $^1\text{H}$  NMR ( $\text{C}_6\text{D}_6$ , 200 MHz)  $\delta$  4.81 ( $\mu_3\text{-CCH}_3$ ), 1.72 ( $\text{CNCMe}_3$ ), 1.64 ( $\text{C}_5\text{Me}_5$ ),  $-27.2$  ( $\mu\text{-H}$ );  $^{13}\text{C}\{^1\text{H}\}$  NMR ( $\text{C}_6\text{D}_6$ , 126 MHz)  $\delta$  92.7 ( $\text{C}_5\text{Me}_5$ ), 58.1 ( $\text{CNCMe}_3$ ), 45.7 ( $\mu_3\text{-CCH}_3$ ), 32.1 ( $\text{CNCMe}_3$ ), 11.1 ( $\text{C}_5\text{Me}_5$ ),  $\text{CNCMe}_3$  and  $\mu_3\text{-CCH}_3$  carbons not observed; HRMS (EI) calcd (found) for  $\text{C}_{37}\text{H}_{58}\text{NC}_3$ :

**Table 5.** Atomic Coordinates for  $\text{Cp}^*_3\text{Co}_3(\mu_3\text{-CCH}_3)(\mu_3\text{-CO})(\mu_2\text{-H})$  (**5**)

	$10^5x$	$10^5y$	$10^5z$	$10^4U(\text{eq})^a$ ( $\text{\AA}^2$ )
Co(1)	52491(4)	30795(5)	25000	316(3)
C(1)	66667	33333	16539(32)	367(14)
O(1)	66667	33333	8194(284)	668(85)
C(2)	66667	33333	7619(394)	562(58)
C(3)	30101(43)	15444(48)	25000	717(23)
C(4)	33531(30)	24173(37)	17585(22)	602(15)
C(5)	39129(28)	38427(33)	20308(21)	551(14)
C(6)	21832(54)	-917(56)	25000	1461(49)
C(7)	30517(49)	18885(58)	8444(30)	1265(34)
C(8)	43034(44)	51091(45)	14563(33)	1062(26)

<sup>a</sup> Equivalent isotropic  $U$  defined as one-third of the trace of the orthogonalized  $U_{ij}$  tensor.

**Table 6.** Atomic Coordinates for  $\text{Cp}^*_3\text{Co}_3(\mu_3\text{-CCH}_3)(\mu_3\text{-CNCMe}_3)(\mu_2\text{-H})\cdot\frac{1}{2}\text{C}_5\text{H}_{12}$  (**6** $\cdot\frac{1}{2}\text{C}_5\text{H}_{12}$ )

	$10^4x$	$10^4y$	$10^4z$	$10^3U(\text{eq})^a$ ( $\text{\AA}^2$ )
Co(1)	1691(1)	9126(1)	7880(1)	32(1)
Co(2)	4280(1)	8300(1)	7906(1)	33(1)
Co(3)	2527(1)	10875(1)	7894(1)	34(1)
C(1)	2523(9)	9805(10)	7078(3)	115(4)
N(1)	2318(10)	10122(11)	6434(3)	181(5)
C(2)	2365(6)	10554(6)	5708(3)	68(3)
C(3)	885(9)	11697(9)	5358(5)	168(4)
C(4)	3371(8)	11145(8)	5591(5)	132(4)
C(5)	2849(9)	9264(9)	5405(5)	140(4)
C(6)	2970(4)	9097(4)	8541(2)	31(2)
C(7)	3148(5)	8669(5)	9344(2)	53(2)
C(8)	1057(5)	7520(5)	7936(3)	51(2)
C(9)	286(5)	8689(6)	7323(3)	54(2)
C(10)	-511(4)	9989(5)	7550(3)	51(2)
C(11)	-252(4)	9601(5)	8316(3)	47(2)
C(12)	715(4)	8072(5)	8544(3)	48(2)
C(13)	1845(6)	5925(6)	7950(4)	99(3)
C(14)	220(8)	8556(9)	6562(3)	105(4)
C(15)	-1559(6)	11481(6)	7064(4)	90(3)
C(16)	-994(6)	10577(6)	8800(3)	82(3)
C(17)	1133(7)	7147(7)	9314(3)	89(3)
C(18)	6519(4)	7601(5)	7966(3)	54(2)
C(19)	6139(4)	7274(5)	7358(3)	51(2)
C(20)	5604(4)	6331(4)	7613(3)	46(2)
C(21)	5689(4)	6053(4)	8376(3)	48(2)
C(22)	6258(5)	6853(5)	8590(3)	52(2)
C(23)	7312(6)	8430(6)	7953(4)	95(3)
C(24)	6448(6)	7689(7)	6607(3)	92(3)
C(25)	5168(6)	5612(6)	7159(3)	77(3)
C(26)	5396(6)	4958(6)	8881(3)	76(3)
C(27)	6699(6)	6729(7)	9354(3)	89(3)
C(28)	951(5)	13043(4)	7930(3)	50(2)
C(29)	1692(5)	13150(4)	7321(3)	49(2)
C(30)	3146(5)	12466(5)	7580(3)	48(2)
C(31)	3311(5)	11973(5)	8351(3)	48(2)
C(32)	1947(5)	12344(5)	8560(3)	49(2)
C(33)	-664(5)	13835(6)	7903(4)	90(3)
C(34)	974(7)	14000(6)	6570(3)	85(3)
C(35)	4333(6)	12422(6)	7141(3)	78(3)
C(36)	4685(6)	11335(6)	8852(3)	76(3)
C(37)	1587(7)	12213(6)	9321(3)	83(3)
C(1S)	5173(47)	4520(35)	5231(20)	279(5)
C(2S)	3723(17)	5402(20)	5006(11)	279(5)
C(3S)	2791(16)	5164(16)	4792(9)	279(5)

<sup>a</sup> Equivalent isotropic  $U$  defined as one-third of the trace of the orthogonalized  $U_{ij}$  tensor.

693.2526 (693.2547). Anal. Calcd (found) for  $\text{C}_{37}\text{H}_{58}\text{NC}_3$ : C, 64.07 (63.88); H, 8.43 (8.17).

**$\text{Cp}^*_3\text{Co}_3(\mu_3\text{-CCH}_3)(\mu_3\text{-NO})$  (**7**).** A solution of NO (0.04 mmol) and **3** (25 mg, 0.04 mmol) in 6 mL of benzene was stirred for 1 h in a 35-mL sealed flask. After filtration through Celite, the benzene was evaporated under vacuum and the residue was washed with pentane to give **7** as a red powder (22 mg, 84%) which was  $>95\%$  pure by  $^1\text{H}$  NMR. **7** was further purified by recrystallization from toluene at  $-20$   $^\circ\text{C}$ :  $^1\text{H}$  NMR ( $\text{C}_6\text{D}_6$ , 200 MHz)  $\delta$  4.43 ( $\mu_3\text{-CCH}_3$ ), 1.53 ( $\text{C}_5\text{Me}_5$ );  $^{13}\text{C}\{^1\text{H}\}$  NMR ( $\text{C}_6\text{D}_6$ , 126 MHz)  $\delta$  92.7 ( $\text{C}_5\text{Me}_5$ ), 44.9 ( $\mu_3\text{-CCH}_3$ ), 9.7 ( $\text{C}_5\text{Me}_5$ ),  $\mu_3\text{-CCH}_3$  carbon not observed; IR ( $\text{CHCl}_3$ ) 1374  $\text{cm}^{-1}$ ; HRMS (EI) calcd

(found) for  $C_{32}H_{48}NOCo_3$  ( $M^+$ ) 639.1729 (639.1737). Anal. Calcd (found) for  $C_{32}H_{48}NOCo_3$ : C, 60.10 (59.99); H, 7.56 (7.51).

**X-ray Crystallographic Determinations and Refinements.** Each crystal was coated in epoxy and mounted on the tip of a thin glass fiber. Diffraction data were obtained with graphite-monochromated Mo  $K\alpha$  radiation on a Siemens P4RA diffractometer at 294–296 K. Automatic indexing of 18–20 well-centered reflections determined the unit cell; precise unit cell dimensions were determined by least-squares refinement of 25 well-centered, high-angle reflections ( $25^\circ < 2\theta < 30^\circ$ ). Empirical absorption corrections were applied to each data set.<sup>24</sup> Initial positions for Co atoms were found by direct methods, and all non-hydrogen atoms were located from successive difference Fourier maps. All non-hydrogen atoms were refined anisotropically; carbon-bound hydrogen atoms were fixed at idealized positions with isotropic thermal parameters of  $U = 0.08 \text{ \AA}^2$ . Co-bound hydrides were not crystallographically observed. Crystallographic computations were performed employing SHELXTL-PLUS<sup>25</sup> software on VAX computers. Final Fourier difference maps revealed no unusual features.

**X-ray Crystallography of  $Cp^*_3Co_3(\mu_3-CCH_3)(\mu_3-CO)(\mu_2-H)$  (5).** Slow evaporation of a toluene solution gave black crystals of **5** suitable for X-ray analysis. Systematic absences and a statistical analysis of the data were consistent with the space group  $P6_3/m$ . Standard reflections showed no significant variations throughout data acquisition. The 2547 reflections collected produced 824 independent, observed reflections ( $|F| > 4.0\sigma(F)$ ). The crystallographic site symmetry ( $3/m$ ) required the disorder of the  $\mu_3-CO$  and  $\mu_3-CCH_3$  ligands. The structure was therefore refined according to a mirror-disorder model which assigned full-weight to a single apical carbon atom (12 electrons) and half-weight to the disordered oxygen atom (8 electrons) and the ethylidyne methyl group (9 electrons). The O(1) and C(2) atoms refined to independent positions along the crystallographic 3-fold axis. Crystallographic data (Table 1), selected bond lengths and bond angles (Table 2), and atomic coordinates (Table 5) are presented.

**X-ray Crystallography of  $Cp^*_3Co_3(\mu_3-CCH_3)(\mu_3-CNCMe_3)(\mu_2-H)$  ( $1/2C_5H_{12}$  ( $6^{1/2}C_5H_{12}$ )).** Slow evaporation of a pentane solution gave black crystals of  $6^{1/2}C_5H_{12}$  suitable for X-ray analysis. Cluster **6** crystallized in the triclinic space group  $P\bar{1}$ ; the unit cell contained two molecules of **6** and one molecule of pentane. The 2547 reflections collected produced 824 independent, observed reflections ( $|F| > 4.0\sigma(F)$ ). Standard reflections displayed a 20% decrease in intensity throughout data acquisition, consistent with loss of pentane from the crystal, and the data were corrected

(24) Empirical absorption corrections were based on  $\psi$ -scan measurements at different azimuthal angles.

(25) SHELXTL-PLUS, Siemens Analytical X-Ray Instruments, Inc.

**Table 7.** Atomic Coordinates for  $Cp^*_3Co_3(\mu_3-CCH_3)(\mu_3-NO)$  (7)

	$10^4x$	$10^4y$	$10^4z$	$10^3U(eq)^a$ ( $\text{\AA}^2$ )
Co(1)	3084(1)	5258(1)	2500	32(1)
C(1)	3333	6667	1705(4)	41(2)
N(1)	3333	6667	1705(4)	41(2)
O(1)	3333	6667	894(37)	67(9)
C(2)	3333	6667	717(63)	67(9)
C(3)	1565(8)	3014(7)	2500	71(3)
C(4)	2421(6)	3365(5)	1768(4)	64(3)
C(5)	3864(5)	3941(5)	2032(3)	59(2)
C(6)	-61(9)	2174(9)	2500	171(9)
C(7)	1910(9)	3101(9)	840(5)	139(6)
C(8)	5149(7)	4363(7)	1460(5)	109(4)

<sup>a</sup> Equivalent isotropic  $U$  defined as one-third of the trace of the orthogonalized  $U_{ij}$  tensor.

accordingly. Crystallographic data (Table 1), selected bond lengths and bond angles (Table 3), and atomic coordinates (Table 6) are presented.

**X-ray Crystallography of  $Cp^*_3Co_3(\mu_3-CCH_3)(\mu_3-NO)$  (7).** Slow evaporation of a toluene solution gave black crystals of **7** suitable for X-ray analysis. Systematic absences and a statistical analysis of the data were consistent with the space group  $P6_3/m$ . Standard reflections showed no significant variations throughout data acquisition. The 2103 reflections collected produced 817 independent, observed reflections ( $|F| > 4.0\sigma(F)$ ). The crystallographic site symmetry ( $3/m$ ) required disorder of the  $\mu_3-NO$  and  $\mu_3-CCH_3$  ligands. The structure was therefore refined according to a mirror-disorder model which assigned full-weight to a single apical atom (13 electrons) and half-weight to the disordered oxygen atom (8 electrons) and the ethylidyne methyl group (9 electrons). The O(1) and C(2) atoms refined to independent positions along the crystallographic 3-fold axis. Crystallographic data (Table 1), selected bond lengths and bond angles (Table 4), and atomic coordinates (Table 7) are presented.

**Acknowledgment.** Financial support from the National Science Foundation and the Department of Energy, Office of Basic Energy Sciences, is gratefully acknowledged. Grants from the NSF (CHE-9105497) and from the University of Wisconsin for the purchase of the X-ray instruments and computers are acknowledged. R.A.W. and S.L.H. thank the Department of Education for fellowships.

**Supplementary Material Available:** Tables of structural determination data, anisotropic thermal parameters for non-hydrogen atoms, interatomic distances and angles, and idealized atomic parameters for hydrogen atoms (18 pages). Ordering information is given on any current masthead page.